Catalysis Today 176 (2011) 441–448

Contents lists available at ScienceDirect

Catalysis Today

journal homepage: www.elsevier.com/locate/cattod

Performances of novel sulfated ceria–zirconia catalysts for the selective catalytic reduction of NOx by ethanol

Alexandre Westermann, Bruno Azambre*

Laboratoire de Chimie et Méthodologies pour l'Environnement (LCME), Institut Jean Barriol, Université Paul Verlaine – Metz, Rue Victor Demange, 57500 Saint-Avold, France

ARTICLE INFO

Article history:
Received 14 September 2010
Received in revised form 18 October 2010
Accepted 19 October 2010
Available online 13 December 2010

Keywords:
NOx
SCR
TPSR
Ceria
Sulfates
Acetaldehyde

ABSTRACT

In this study, sulfated ceria–zirconia (SCZ) catalysts with increasing Ce molar fractions (xCe = 0; 0.21; 0.5; 0.75 and 1) were prepared by direct sulfation of the crystallized CZ nanopowders in 0.5 M H_2SO_4. As revealed by XRD and TGA, the sulfation treatment created surface sulfates with a density of 2–3 SO_4^{2-}/nm^2 whatever the Ce content while maintaining the original crystalline structure of the CZ material. The investigation of ethanol-SCR performances under (1920 ppm NO + 3020 ppm C_2H_5OH + 5% O_2) TPSR and steady-state conditions allowed to obtain N_2 yields superior to 45% on the most active SCZ catalysts around 350–400 °C. Catalytic results relative to the sulfated and non-sulfated catalysts are then discussed according to the Ce molar fraction and the CZ structure. The possible reaction pathways involved in the formation/decomposition of some important SCR intermediates such as ethylnitrite, acetaldehyde, HCN and NH_3 are examined on the basis of the collected TPSR data.

© 2010 Elsevier B.V. All rights reserved.

1. Introduction

The selective catalytic reduction (SCR) by ammonia is considered as a mature technology for the abatement of nitrogen oxides (NOx) generated from stationary sources [1]. However, NH_3-SCR presents some drawbacks in the automotive field which are namely associated with the storage, handling or even the disposal of the reductant [2]. These problems are partially overcome by using urea as the ammonia source and urea-SCR is currently being considered as the primary NOx control technology for meeting the future emission standards by many automakers worldwide [3,4]. Nevertheless, the alternative use of hydrocarbons (HCs) as reductants still remains attractive because these species are found directly in the exhaust gases [5–10]. In that respect, both the catalysts durability in wet streams and the DeNOx yields have to be improved to make the HC-SCR process a cost-effective technology. The reductant efficiency in the NOx reduction to N_2 usually follows the order: alkanes < alkenes < oxygenated [5]. In that respect, ethanol is interesting for mobile applications because on the one hand, it can be produced from renewable energy sources and mixed with diesel fuel and on the other hand, it is less toxic than ammonia. Moreover, ethanol was found to be one of the most active and selective reductants over the widely-studied Ag/Al_2O_3 catalyst but also on Ag-, Na- or Ba-Y zeolites [5,11–13]. These catalysts generally display an excellent activity at medium–high temperatures but challenges relevant to unwanted products (HCN, ammonia, acetaldehyde) produced under some conditions and insufficient activity at low temperatures still need to be solved [5,11–13].

By contrast, little attention has been paid to ceria-based catalysts in HC-SCR processes [14,15], in spite of their well-known redox properties [16]. This is probably because of the high oxidizing ability of the Ce^{4+}/Ce^{3+} couple, which is thought to promote more the hydrocarbon combustion than the NOx reduction under lean conditions. However, ceria can also be sulfated [17], which allows in principle to tune both the acid-base and apparent oxygen storage capacities (OSCs) properties of sulfated ceria–zirconia catalysts. Recently, we have reported an extensive characterization of some selected sulfated ceria–zirconia (SCZ) materials obtained by direct sulfation of the crystallized parent nanopowders in sulfuric acid [18]. By comparison with the corresponding non-sulfated CZ materials, the sulfated ones were found to display an increased Lewis and Brönsted acidity and a restricted O mobility, making them interesting as supports or catalysts for CH_4-SCR [19].

In this study, the performances in ethanol-SCR of these novel sulfated ceria–zirconia catalysts are examined according to their composition/structure and compared with those of a conventional ceria–zirconia catalyst. The conditions of formation of important SCR intermediates produced during temperature-programmed surface reactions (TPSRs) and steady-state experiments are investigated to establish structure-properties relationships and to unravel the SCR mechanism.

* Corresponding author. Tel.: +33 387939106; fax: +33 87939101.
E-mail address: bazambre@univ-metz.fr (B. Azambre).

0920-5861/$ – see front matter © 2010 Elsevier B.V. All rights reserved.
doi:10.1016/j.cattod.2010.10.071

Table 1
Textural, chemical and structural characteristics of sulfated ceria-zirconia catalysts.

Catalysts	Specific surface area (m^2/g)	Surface density of sulfate groups (SO_4^{2-}/nm^2)	DTG_{max} during sulfate desorption (°C)	Crystal phase (XRD/Raman)[a]	Crystal size (nm)[b]
CeO_2 sulfated (SC)	284	2.5	781	c	12
$Ce_{0.8}Zr_{0.2}O_2$ sulfated (SCZ82)	185	2.7	751	c	6
$Ce_{0.5}Zr_{0.5}O_2$ sulfated (SCZ55)	87	2.0	889	t′ + t″ (c and m)	7
$Ce_{0.2}Zr_{0.8}O_2$ sulfated (SCZ28)	184	2.0	910	t (and m)	3
ZrO_2 sulfated (SZ)	22	3.2	912	m	25

[a] c = cubic, t, t′, t″ = tetragonal phases, m = monoclinic.
[b] As computed from the Debye-Scherrer equation.

2. Experimental

2.1. Catalyst syntheses

$Ce_xZr_{1-x}O_2$ (CZ) nanopowders with $x = 0$, 0.2, 0.5, 0.8 and 1 were kindly supplied by Rhodia (La Rochelle, France). Sulfated ceria–zirconia catalysts (SCZs) were obtained by: (i) reacting the crystallized CZ material (5 g) with a 0.5 M H_2SO_4 solution (100 mL) for 45 min; (ii) washing the slurry with diluted 0.05 M H_2SO_4; (iii) drying at 70 °C under vacuum for 24 h and calcination in air at 500 °C for 2 h. In the following, they are labeled according to their relative content in Ce and Zr. For instance, a catalyst labeled SCZ28 indicates Ce and Zr molar fractions of 0.2 and 0.8, respectively.

2.2. TPSR and isothermal ethanol-SCR tests

Temperature-programmed surface reactions (TPSRs) and steady-state isothermal experiments were carried out in a tubular quartz reactor itself placed in a Carbolite MTF furnace regulated with a Eurotherm temperature controller. Standard conditions for ethanol-SCR tests were 1920 ppm NO + 3020 ppm C_2H_5OH + 5% O_2 (He balance); $m_{catalyst}$ = 0.2 g; GHSV = 50,000 h^{-1}. Certified gases (NO/He, NO_2/He, O_2 and He) were fed from compressed cylinders provided by Air Liquide and their concentrations were adjusted with Brooks 5850S mass-flow controllers. Constant ethanol concentration (calculated from Antoine coefficients) was supplied to the reacting stream by means of a bubble tower purged by He flow and immerged in a thermostated bath at 2 °C (accuracy ±0.1 °C). Before reaching the catalyst bed (consisting of the pelletized catalyst powder crushed and sieved to 0.5–1 mm and two quartz wool plugs), all the feed gases were allowed to pass through a home-made glass mixture chamber for further dilution and better homogeneity of the reacting stream. The composition of the reactor outflow was continuously monitored using a heated FTIR gas cell (Cyclone Series – Specac, optical path length = 2 m, V = 0.19 L) coupled to a Varian Excalibur 4100 FTIR spectrometer with a DTGS detector. The temperature of the gas cell was maintained at 110 °C to avoid any condensation of the reactants/products during the tests. FTIR spectra, referenced to a He background, were recorded using a 2 cm^{-1} resolution and co-addition of 50 scans. These parameters allowed to obtain satisfying signal/noise ratio as well as a sufficient time resolution (the sampling rate was 1 spectrum per 5 °C intervals during the TPSR) but also to detect the fine gas structure in most cases for identification purposes.

Prior to catalytic tests, the catalysts were pre-treated from 25 to 500 °C under 5%O_2 in He (v = 20 °C min^{-1}) to remove most of adsorbed impurities. After cooling down to 30 °C (under He), the standard gas mixture was sent through the catalyst and the temperature was ramped from 25 to 500 °C (TPSR experiments, v = 5 °C min^{-1}). Then, the temperature was decreased progressively from 500 to 150 °C by dwells of 50 °C to measure the SCR activity of the catalysts under steady-state conditions (in our conditions after 1 h at each temperature). On the whole set of catalytic experiments, up to 22 different N- and C-compounds were detected and identified using different FTIR spectral libraries. 10 compounds (ethanol, acetaldehyde, ethene, CO, CO_2, ethylnitrite, NO, NO_2, N_2O and NH_3), among the most important ones in terms of amounts sent/produced (with the exception of HCN that could not be accurately calibrated), were quantitated from their areas or absorbances in FTIR spectra using certified standards or other methodologies. Complex signal treatment procedures using different steps of spectral subtractions were often required to get rid of spectral interferences between some compounds. The quantification accuracy was checked systematically using C- and N-balances. In most cases, the sum of the computed concentrations closely corresponded to the concentrations of the C- and N-feeds.

2.3. Characterization studies

X-ray diffraction (XRD) analyses were carried out thanks to a Bruker-AXS diffractometer with the CuKα radiation (1.5405 Å). Powdered diffraction patterns were recorded between 20 and 65° (2θ) using increments of 0.01° and a counting time of 0.1 s.

Specific surface areas were obtained using N_2 adsorption isotherms recorded at 77 K and the BET method.

The surface densities of sulfate species grafted on the SCZ materials during the treatment with sulfuric acid and their thermostabilities were determined using a Mettler-Toledo TGA/SDTA851e thermogravimetric (TG) analyzer. The heating program consisted of heating the catalysts (50 mg) under Ar flow (60 mL min^{-1}) from 25 up to 1200 °C (v = 10 °C min^{-1}). Surface densities were obtained from: (i) the computation of mass losses due to the decomposition of sulfates to SO_2 [18] above 600 °C; (ii) subsequent normalization by the specific surface area of each catalyst (N_2 adsorption at 77K, BET method).

3. Results and discussion

3.1. Characterization of SCZ catalysts

3.1.1. Structural and textural characterization

A detailed phase analysis by XRD and Raman spectroscopy of the parent (non-sulfated) CZ materials had been performed previously [20]. From Fig. 1A and [20], it can be deduced that the XRD patterns of the sulfated SCZ catalysts investigated in the present study are similar to those of their parent CZ materials. The crystalline phases present in the different SCZ materials are reported in Table 1. They will not be commented in details for each composition for the sake of brevity. Nevertheless, the absence of new peaks in XRD patterns indicates that bulk sulfate phases (such as those obtained when cerium and zirconium hydroxide precursors are sulfated [21]) are not formed when the sulfation treatment is performed onto CZ materials which are already crystallized. Being a surface treatment only, the sulfation does not significantly affect the crystallite size nor than the specific surface area (Table 1 and [20]). However, it strongly modifies the acid-base and redox properties and consequently the catalytic behaviour [18]. Rather similar conclusions were drawn when the structural and catalytic proper-

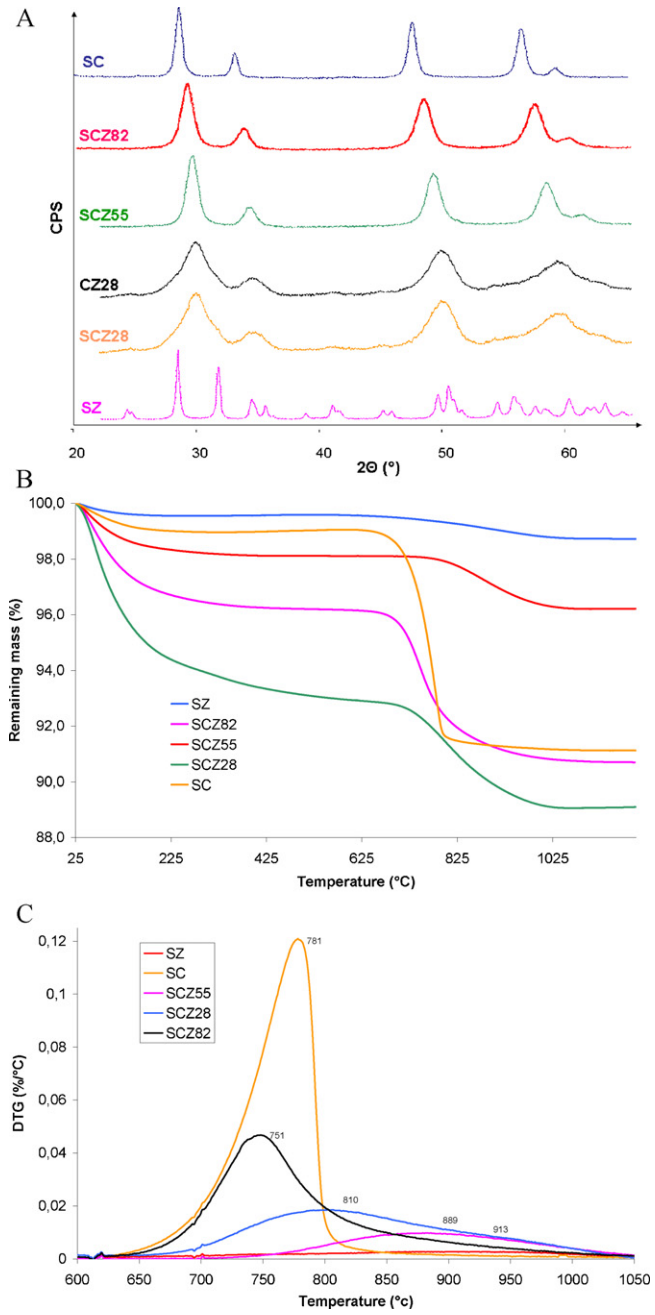

Fig. 1. Characterization of the catalysts by XRD and TGA. (A) XRD patterns of SCZ and CZ catalysts; (B) TGA curves corresponding to the heating of the SCZ catalysts under Ar from 25 to 1200 °C (v = 10 °C/min); (C) Derivatives (DTG) of the TG curves displayed in (B).

ties of sulfated zirconia catalysts prepared by different methods were compared [22].

3.1.2. Thermal behaviour of sulfate species grafted on SCZ materials

Results obtained following the TG analysis of sulfated (SCZ) supports are presented on Fig. 1B and C. As deduced from TG curves (Fig. 1B) and their derivatives (DTG, Fig. 1C), the sulfate species existing on the different SCZ materials after the treatment of the parent CZ with H_2SO_4 are stable at least up to 600 °C under inert atmosphere before they start decomposing to SO_2 [18]. As deduced from Table 1, sulfated materials have rather comparable SO_4^{2-} surface densities, of the order of 2–3 SO_4^{2-}/nm^2, whatever the Ce content and despite very different specific surface areas. This shows that sulfate species probably did not anchor preferentially on Ce or Zr sites during the treatment with sulphuric acid in line with the fact that both ceria and zirconia can be sulfated. Nevertheless, the thermostability of these sulfate species was found to be strongly dependent on the composition/structure of the parent $Ce_xZr_{1-x}O_2$ materials. Indeed, the regular increase of the peak temperature on DTG curves (Fig. 1C) with the Zr content indicates that sulfate species anchored to Zr sites are generally more thermally stable than those on Ce sites. A rather similar conclusion was drawn when the relative thermostability of adsorbed nitrate species was considered in our previous studies [23]. The present results can be explained both by the known superior Lewis acidity of Zr^{x+} cations, which enhances the strength of the surface sulfate complexes, and/or to the redox properties of cerium, which may promote its decomposition to SO_2 at lower temperatures. Moreover, the delayed onset of sulfates desorption for the SCZ55 catalyst compared with the SC material point out additional effects brought by the exposed surface structures. In the rich literature existing on sulfated zirconia materials [22,24], it has been proposed than sulfates located on terrace sites are more stable than those on defective sites, such as steps, kinks and corners. Hence, the variations observed in the width of DTG peaks (Fig. 1C, and/or the relative steepness of the mass losses observed on TG curves (Fig. 1B)) are indicative of the relative heterogeneity of the anchoring surface sites, i.e. the types of surface structures present on the different materials. According to Fig. 1C, Zr-rich surfaces and tetragonal structures are much more heterogeneous than Ce-rich ones, the sulfated ceria (SC) material with cubic fluorite structure displaying clearly the most uniform surface sites. In that respect, it is known that the insertion of Zr in ceria creates point or clustered defects (often associated with O vacancies), which may promote the preferential growth of new surface planes or local distorted surface structures [16]. Hence, the grafted sulfate species have to accommodate the local geometrical constraints brought by the different surface structures and this is clearly reflected on TG and DTG curves.

3.2. Gas-phase chemistry – blank TPSR experiments

The nature of the reactions occurring in the gas phase when ($NO_2 + C_2H_5OH$) or ($NO + O_2 + C_2H_5OH$) mixtures were heated from 35 to 500 °C is revisited in this section. We judge it necessary because: (i) depending on the temperature, part of the ethanol may already have been partially transformed to primary or secondary products (as we will see) by reactions involving radicals in the hot zone of the reactor before penetrating the catalyst bed. Hence, the amounts of ethanol really seen by the catalyst would probably be inferior to that expected from the feed composition and this can affect the DeNOx temperatures windows and yields; (ii) our results showed some discrepancies with some of the data already existing in the literature [25], which may possibly be related to some differences existing in the setup used or the reaction conditions.

3.2.1. TPSR under ($NO_2 + C_2H_5OH$)

The evolution of C- and N-compounds, deduced from the quantitative exploitation of FTIR spectra recorded during the non-catalyzed ($NO_2 + C_2H_5OH$) TPSR reaction, is displayed in function of the temperature on Fig. 2A and B, respectively. Starting from 35 °C, it is observed that about 40% of the initial NO_2 reacts with ethanol to yield ethylnitrite and nitric acid (the latter was not quantitated due to multiple adsorptions in the analytical system) according to following reaction:

$$2NO_2 + EtOH \rightarrow EtONO + HNO_3 \quad (1)$$

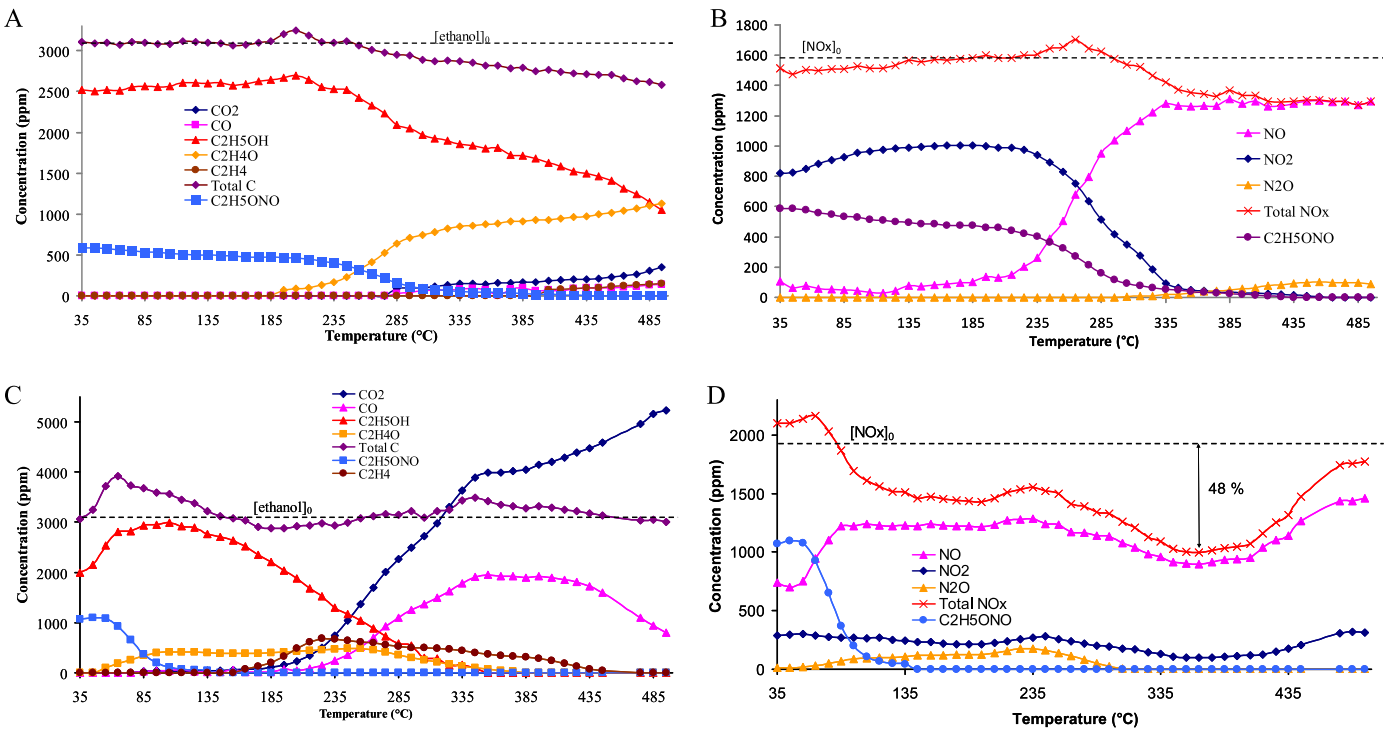

Fig. 2. TPSR profiles measured between 35 and 500 °C (ν = 5 °C/min) under selected conditions. Evolution of C-products (A) and N-products (B) in the course of the non-catalyzed (1590 ppm NO_2 + 3020 ppm ethanol) experiment; evolution of C-products (C) and N-products (D) in the course of a catalyzed (1920 ppm NO + 3020 ppm ethanol + 5% O_2) experiment over the SCZ28 catalyst.

Above 135 °C, the ethylnitrite produced by Eq. (1) starts to decompose slowly to NO, ethanol and acetaldehyde, with the following stoichiometry, as deduced from TPSR profiles and [11]:

$$4C_2H_5ONO \rightarrow 3C_2H_4O + 2NO + C_2H_5OH + N_2O + H_2O \quad (2)$$

The severe drop in the NO_2 concentration observed from 200 °C, accompanied by the production of NO and acetaldehyde, is indicative of another reaction, which becomes progressively preponderant over Eq. (2) above 250 °C:

$$C_2H_5OH + NO_2 \rightarrow CH_3CHO + NO + H_2O \quad (3)$$

Above 285 °C, a fraction of the ethanol and the acetaldehyde produced in Eqs. (2) and (3) becomes partly oxidized to CO, CO_2 and other minor products (methanol, formaldehyde, ethene). The detection of small amounts of HCN, HNCO, N_2O and N_2 (as deduced from the negative N-balance) in the 400–500 °C range indicates that NOx reduction takes also place in the gas phase.

3.2.2. TPSR under ($NO + O_2 + C_2H_5OH$)

Substituting the ($NO_2 + C_2H_5OH$) mixture by the "standard" ($NO + O_2 + C_2H_5OH$) one led sensibly to the same observations at the low-medium temperatures (up to 300 °C). This seems reasonable considering that: (i) some NO_2 is produced by NO oxidation even in the absence of catalyst; and (ii) the oxidizing power of NO_2 is by far superior to that of O_2. Hence, NO_2 is the main oxidizing agent in the system up to 300 °C. At higher temperatures, the oxidation of ethanol and some its transformation products (acetaldehyde, ethene, CO) by O_2 become the preponderant phenomenon, as revealed by the important CO_2 emissions detected (75% of the sum of all C-products at 500 °C). Also worth noting, the decomposition rate of ethylnitrite to acetaldehyde (Eq. (2)) was increased in the presence of O_2.

To sum up, the study of the gas-phase chemistry allowed to establish that a part of the ethanol in the ($NO + O_2 + C_2H_5OH$) feed is transformed to: ethylnitrite at low temperatures (about 20% in the 35–180 °C range); acetaldehyde (from 15 to 40% in the 200–500 °C range, peaking around 400 °C) and ethene (20% around 430 °C) at medium–high temperatures; CO_2 at the high temperatures (from 10 to 75% in the 370–500 °C range). In the presence of a catalyst, the gas-phase reactions leading to these products are believed to be less significant because the residence times would be somewhat decreased. Nevertheless, acetaldehyde being known as an efficient reductant, its production by gas-phase reactions is expected to promote (or at least not lower) the SCR activity of the catalysts at medium–high temperatures whereas the presence of CO_2 at the highest temperatures would have an opposite effect.

3.3. Ethanol-SCR activities of the SCZ and CZ catalysts

3.3.1. General description of catalyzed TPSR experiments

In this section, the evolution of C- and N-compounds according to the temperature is first commented for the SCZ28 catalyst. It has to be outlined that the TPSR data measured for the other SCZ catalysts were rather comparable, differing only slightly by the amounts of each species detected and the temperature at which the transformations took place. Because the same trends prevail, we will consider in the following the SCZ28 material as a representative example of a SCR-active sulfated catalyst. Its TPSR profiles under "standard SCR conditions" ($NO + O_2 + C_2H_5OH$) are given on Fig. 2C and D, respectively. By comparison with the non-catalyzed conditions, the addition of the SCZ catalyst markedly increased the reactivity of the system, as expected. At 35 °C (Fig. 2C and D), the amount of ethylnitrite produced is twice that detected under non-catalyzed conditions, even when a ($NO_2 + C_2H_5OH$) mixture was used (Fig. 2A and B) instead of the standard ($NO + O_2 + C_2H_5OH$) conditions (not shown). Therefore, these results can not be regarded as solely due to an enhanced NO_2 production (from NO oxidation) by the sulfated catalyst (Eq. (1)). Preliminary DRIFTS experiments have shown that both NOx and ethanol are readily adsorbed on the catalysts at room temperature. Hence, it seems likely, that a

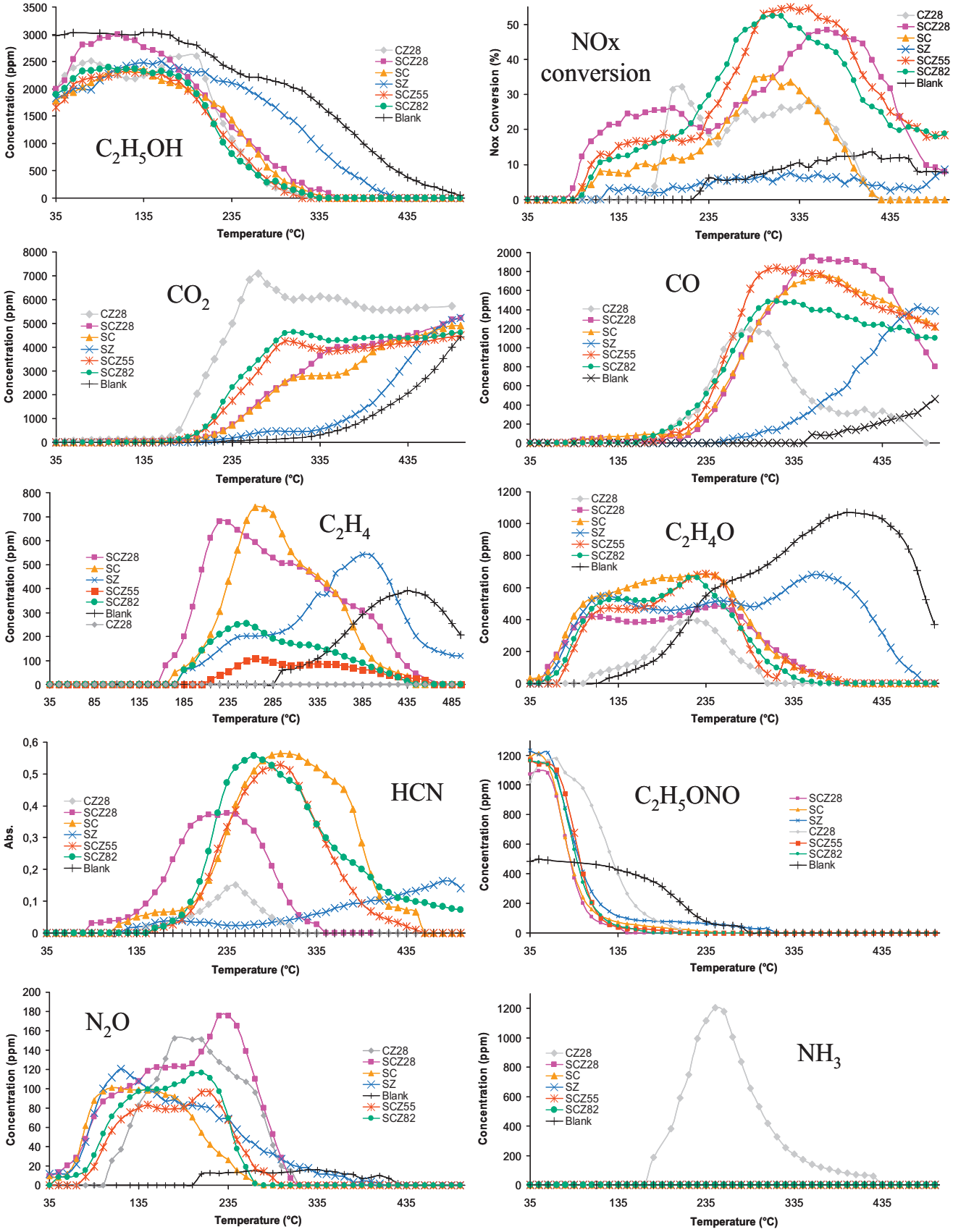

Fig. 3. Comparison of the individual TPSR profiles of ethanol, NOx, CO, CO_2, C_2H_4, C_2H_4O, HCN, C_2H_5ONO, N_2O, and NH_3 measured under standard (1920 ppm NO + 3020 ppm ethanol + 5% O_2) conditions between 35 and 500 °C (ν = 5 °C/min) for the different SCZ and CZ catalysts. (For interpretation of the references to color in this figure legend, the reader is referred to the web version of the article.)

surface pathway is operative for the formation of ethylnitrite during the catalyzed NO_2–ethanol reaction (Eq. (1)). The mechanism is not beyond the scope of this study but should at least involve one surface reaction between a gaseous or adsorbed form of NO_2 (presumably nitrites [20,23]) and ethanol or an adsorbed ethoxy species [11]. On the other hand and because of its adsorption on the catalyst, nitric acid was not detected in catalyzed experiments though it is expected to be produced simultaneously to ethylnitrite (Eq. (1)). According to Le Châtelier's law, the trapping of HNO_3 on the surface may push the equilibrium towards the formation of ethylnitrite, which also explains the results. Second, the ethylnitrite decomposition to NO, N_2O acetaldehyde and ethanol (Eq. (2)) is observed at much lower temperatures than on non-catalyzed conditions (55 °C against 130 °C, Fig. 2). These results show that the SCZ28 material is able to catalyze both the production and decomposition of ethylnitrite (Eqs. (1) and (2), respectively). The onset of ethanol consumption is detected at 105 °C for the SCZ28 catalyst (against 280 °C under non-catalyzed conditions) and this process is accompanied by the production of acetaldehyde, which is the major C-product up to 200 °C (Fig. 2C). Ethene is also detected from 165 °C (peak at 230 °C) following the depletion of the diethylether (not reported on Fig. 2C, but revealed by the presence of a strong band at 1120 cm^{-1} in FTIR spectra) already formed at lower temperatures. As we will see, the latter products were never observed in presence of the non-sulfated CZ28 catalyst (Fig. 3). According to our previous study [18], the sulfation by H_2SO_4 has brought some Brönsted acidity on the ceria–zirconia surface, which has rather basic character [26]. Hence, this points out the participation of Brönsted acid sites to the dehydration reactions leading to ethene, which can be globally depicted by Eq. (4):

$$2\,C_2H_5OH \rightarrow C_4H_{10}O + H_2O \rightarrow 2C_2H_4 + H_2O \quad (4)$$

Above 230 °C (Fig. 2C and D), the major process is the strong increase of the NOx conversion simultaneously to the production of CO and CO_2 and the progressive depletion of acetaldehyde and ethene. At 350 °C, both the NOx and ethanol conversions reach their maximal values (48 and 100%, respectively) and acetaldehyde is almost completely depleted. Above this temperature, the NOx conversion decreases, exhibiting the typical volcano-shaped curve of SCR catalysts, whereas the production of CO_2 still increases, however with a lower rate. Classically, these results show that, below 350 °C, the rate of the SCR reaction is higher than the rate of the non-selective combustion of the hydrocarbon species by O_2. On the high-temperatures side of the DeNOx window, combustion reactions become more and more preponderant and the SCR reaction is progressively inhibited. These two reactions can be depicted by (Eq. (5), SCR) and (Eq. (6), combustion), respectively, where $C_xH_y(O)$ represents indifferently ethanol or another reductant present in the system:

$$C_xH_y(O) + 2NO + zO_2 \rightarrow N_2 + x(CO_2, CO) + y/2H_2O \quad (5)$$

$$C_xH_y(O) + zO_2 \rightarrow x(CO_2, CO) + y/2H_2O \quad (6)$$

Because reduced N-products different from N_2 (typically N_2O and HCN for the sulfated catalysts) were detected only at temperatures below 335 °C (Figs. 2D and 3), the NOx conversion measured above this temperature is expected due solely to the formation of N_2 (48% at 350 °C). Since most of the above comments also prevailed for the other SCZ compositions used in this study, this demonstrates that sulfated ceria–zirconia catalysts are rather effective and selective catalysts for ethanol-SCR.

An important issue arises now about the nature of the *true* reductants in our system. In the ethanol-SCR literature [5,11], it is reported that both ethanol and even more likely its partially oxidized product, i.e. acetaldehyde, are effective reductants. On Fig. 2C, the depletion of these compounds simultaneously to the rapid increase of the NOx conversion seems to confirm this. This can also be paralleled with the fact that maximal DeNOx yields are often obtained at temperatures corresponding to 90–100% of the reductant consumption [5]. In that respect, the acetaldehyde formed at medium/high temperatures by gas-phase reactions (see Section 3.1.1 and Fig. 3, blank) may also provide an alternative pathway to increase the DeNOx yield at higher temperatures. Nevertheless and due to the complexity of the system, it is also possible that hydrocarbons different from acetaldehyde and ethanol may participate as reductants in the SCR process. According to TPSR data, these other potential reductants could be ethene and CO but also minor products such as methanol and formaldehyde (not shown on Figs. 2 and 3), which were also detected in FTIR spectra around DeNOx temperatures. Though it is admitted that alkenes are less reactive and SCR-selective than oxygenated hydrocarbons [5], the contribution of ethene as reductant in the system could be envisaged mainly at higher temperatures (typically around 400 °C), i.e. at temperatures where ethanol/acetaldehyde are more rapidly oxidized by O_2 than ethene. More investigations are needed to fully elucidate the role played by each reductant under our conditions.

3.3.2. *Effect of the sulfation on the reactivity*

The changes induced by the sulfation treatment on the reactivity are discussed now. Some of the effects induced by sulfation can be deduced from the comparison of the TPSR profiles (Fig. 3) obtained for the CZ28 (grey curves) and SCZ28 catalysts (pink curves) of similar composition.

Starting from room temperature, it is remarkable that the decomposition of ethylnitrite (Eq. (2)) proceeds at higher temperature on the conventional CZ28 catalyst (onset at 95 °C) than on the sulfated ones (55–65 °C whatever the Ce content). By comparing the decomposition rates of ethylnitrite on various catalysts, it was proposed that the decomposition is not site-specific but depends mostly on the specific surface area [11]. Indeed, this assumption is not confirmed by the present data. Rather, this demonstrates the primary role played by the sulfation treatment and the induced acidity in the decomposition process. In the SZ literature [27], it was proposed that the protons linked either to a bisulfate species or a OH group having acidic properties (in the vicinity of a sulfate species) could promote the activation of hydrocarbons through the formation of carbocations intermediates. Hence, a change in the reaction mechanism is expected to be the main reason why the activation energy relevant to the decomposition of ethylnitrite is lowered for the sulfated catalysts. As a consequence from the delayed ethylnitrite decomposition, less N_2O (Eq. (2)) is produced for the CZ28 catalyst at the low temperatures, which mostly explains the lower NOx conversion measured below 180 °C (Fig. 3).

Though the sulfated and non-sulfated catalysts displayed approximately similar ethanol conversions with the temperature (Fig. 3), they did not make the same use of the hydrocarbon reductant, as expected. On the one hand, the Brönsted acidity brought by sulfation promoted the production of dehydration products, as already discussed in the previous section. On the other hand and in line with the well-known OSC properties of ceria–zirconia materials [16], the conventional CZ28 catalyst promoted the total oxidation of ethanol to CO_2 at temperatures lower than the SCZ28 catalyst does. As a consequence, the NOx reduction window is also limited to a narrower range of temperatures until the complete depletion of the SCR-active reductants takes place. By contrast for the sulfated SCZ28 catalyst, total oxidation was partly inhibited up to 350 °C (as deduced from the inflection points observed on the CO_2 and NOx conversion profiles) and products of mild oxidation (aldehyde, CO, methanol, formaldehyde) or dehydration (ethene, diethylether, acetylene) were formed instead. Hence, the NOx reduction window is broadened towards the high tempera-

tures for the sulfated catalysts and some DeNOx is still observed up to 500 °C (Fig. 3).

The sulfation also strongly influenced the production of potential SCR intermediates involved directly in the formation of N_2. In the literature [5,11,28], the nature of the possible intermediates has been discussed by different authors and the role of HCN and NH_3 has been outlined. On the SCZ catalysts, HCN (Fig. 3 and to a small extent HNCO, not shown), was detected in rather large amounts (estimated as hundreds of ppm but displayed in absorbance scale on Fig. 3). By contrast, ammonia, was not detected over the whole temperatures range whereas significant amounts were observed for the non-sulfated CZ28 catalyst (Fig. 3). According to the studies by Sachtler [11–13], the production of these intermediates on the active Ag/Al_2O_3, Ag-, Ba- and Na-Y catalysts may involve some reactions between NO_2 and adsorbed acetate (produced by acetaldehyde activation) or methyl species (produced from acetyl decomposition) to yield nitromethane or its aci-anion $CH_2{=}NO_2^-$. These very reactive species then dissociate to yield adsorbed CN^- and CNO^- species [11], which in our case readily react with the protons on SCZ surfaces to yield HCN (and HNCO). Depending on the catalysts properties, the species present in the reaction medium and the temperature, the latter compounds can be either oxidized directly to N_2 or hydrolyzed in presence of water to yield NH_3 [28]. As in the fast ammonia-SCR process, the latter will further react in presence of NO to form ammonium nitrite, which decomposes easily to N_2 [28]. In our opinion, the detection of HCN (an acid) and NH_3 (a base) in the gas phase during TPSR experiments depends not only of the intrinsic reactivity of the system but also of the peculiar acid-base properties of the catalysts. Because TPSR profiles represent the net balance between the amounts formed and reacted, it is possible that NH_3 was also produced on the SCZ catalysts but remained in the adsorbed state due to its strong interaction with Lewis and Brönsted acid sites present on the sulfated ceria–zirconia surface. Hence, ammonia is not observed in the gas-phase during TPSR experiments. Instead, the ammonium NH_4^+ species on Brönsted sites rapidly react with NO_2 or a nitrite species providing a pathway for the formation of NH_4NO_2, and finally N_2. On the non-sulfated CZ catalyst, ammonium species are not formed because of their basic and oxidizing character [26] and the fast NH_3-SCR pathway do not apply. Because HCN was detected for all the catalysts and some DeNOx was also obtained with the CZ28 catalyst, it is also possible that part of the N_2 may arise from other channels. One obvious channel is the direct oxidation of HCN and ammonia by NOx and/or O_2 [28]. According to the fact that HCN and ammonia are mainly detected at low/medium temperatures and quickly decline above 250–300 °C, this may be the dominant pathway for the CZ28 catalyst. Hence, the well-known oxidizing properties of ceria–zirconia materials will promote the mild oxidation to N_2 in a narrow temperature range, but at higher temperatures, HCN and NH_3 may be more likely over-oxidized, yielding again NOx in the gas phase [28]. More information will be given in a forthcoming study devoted to the influence of the feed composition and the DRIFTS analyses of adsorbed intermediates under SCR conditions.

3.3.3. *Effect of the Ce content on the SCR activity and the nature of active sites*

The temperature-dependence of the main evolved species during the ($NO + O_2 + C_2H_5OH$) TPSR experiments is compared for the different SCZ catalysts on Fig. 3. NOx conversions were also measured under steady-state conditions (Fig. 4A) to get rid of adsorption/desorption processes. The correlations existing between the maximal NOx conversion, the DeNOx temperature and the Ce content of the catalysts are given on Fig. 4B.

As a rule for the catalysts investigated in this study, the measured conversions in steady-state mode (Fig. 4A) were generally

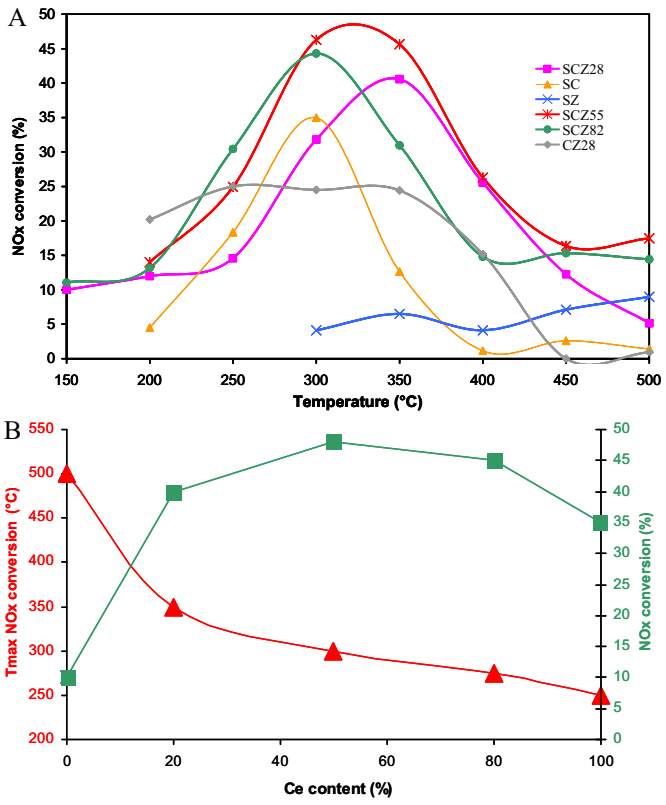

Fig. 4. Summary of isothermal SCR experiments performed under (1920 ppm NO + 3020 ppm ethanol + 5% O_2) conditions on the SCZ and CZ catalysts. (A) Steady-state isothermal NOx conversions in function of the reaction temperature; (B) temperatures of maximal NOx conversions (left) and maximum NOx conversions (right) expressed in function of the Ce molar fraction of SCZ catalysts.

very close to those under TPSR conditions (Fig. 3). This shows that the SCZ catalysts were not deactivated under SCR conditions, at least for the time period investigated. As deduced from Fig. 4, three important observations can be put forward: (i) the first is that the NOx conversion is maximal for a Ce molar fraction of about 0.5 (48% conversion on SCZ55) and this composition also corresponds to the broader DeNOx window. Higher amounts of Ce tend to slightly decrease the yield (35% for the sulfated ceria (SC) catalyst), whereas sulfated zirconia (SZ) is almost completely inactive (<10%, of the same order than blank experiments); (ii) the second point is the regular decrease of the DeNOx temperature with the Ce content of the SCZ catalyst (Fig. 4B). This decrease seems almost linear for Ce molar fractions between 0.2 and 1 but the SZ catalyst is out of the trend; and (iii) under steady-state conditions, the amounts of HCN produced increased with the Ce content (Fig. 3).

From these observations, it appears that both the sulfation treatment and the presence of Ce are required to obtain a reasonable SCR activity. However, this seems not to be sufficient conditions because: (i) otherwise the maximal activity would be obtained for the SC catalyst and not for the SCZ55 one; (ii) the sulfate coverage, as deduced from TGA, is roughly similar for all the catalysts (of the order of 2–3 SO_4^{2-}/nm^2). Hence, the intrinsic SCR activity of Ce sites is probably linked to the peculiar site structure. In Secion 3.1, it was shown that the thermostability of sulfate species exhibited a complex dependence with the Ce molar fraction and the surface structure of the CZ material, the latter being itself affected by the bulk properties and thermal history. In that respect, it is interesting to note that the maximal SCR activities were obtained for Ce molar fractions around 0.5 (typically between 0.2 and 0.8). This also corresponds to the domain where ceria–zirconia materials generally display the highest OSC, i.e. the best redox properties [16]. In

the present study, both tetragonal (SCZ28 and SCZ55) and cubic (SCZ82 and SC) phases were found to be active in ethanol-SCR, but tetragonal ones behaved slightly better. On the other hand, our SZ catalyst (prepared by sulfation of monoclinic ZrO_2) was found to be fairly inactive, which is in line with the fact that a stable tetragonal zirconia phase is a necessary structural condition to obtain active sulfated zirconia catalysts for the isomerization of *n*-alkanes [22]. Though more investigations are needed to confirm this point, it seems also possible that the same rule also applied to SCZ catalysts.

The characterization of some selected (SCZ28 and SCZ73) sulfated ceria–zirconia catalysts by TPD and DRIFTS of adsorbed pyridine [18] had shown that the sulfation treatment increased the acidity of Lewis acid sites and creates some Brönsted acidity in the material. Unfortunately, it was not possible to assess in detail the effects induced by the Ce molar fraction and/or the CZ structural properties because spectroscopic data revealed almost identical features for the two catalysts investigated [18]. Taking into account all the above-mentioned observations, it is proposed that the active site for the reduction of NO (Eq. (5)) may be $[Ce(O,Zr)_n\cdots H]^{x+}$ adducts in the vicinity of a sulfate or bisulfate species. These SCR active species may be located either at the edges/border of the surface planes or at the interfacial area which delimits different nanocompositional domains within the ceria–zirconia crystallites, as suggested by Mamontov when investigating the origin of the OSC in a $Ce_{0.5}Zr_{0.5}O_2$ material [29]. By contrast, active sites for the combustion reaction (Eq. (6)) are likely to exist on portions of the surfaces which are not covered by sulfate species.

4. Conclusions

Novel acidic sulfated ceria–zirconia (SCZ) catalysts with increasing Ce molar fractions (*x*Ce = 0; 0.21; 0.5; 0.75 and 1) were prepared by direct sulfation of the crystallized CZ nanopowders in 0.5 M H_2SO_4. XRD analyses revealed that the crystalline structures of the parent CZ materials were left unchanged by the sulfation treatment. By TGA, it was established that the relative thermostabilities of the grafted sulfate species (with a nominal density of 2–3 SO_4^{2-}/nm^2 on all SCZ materials) showed a complex dependence with the Ce molar fraction of the CZ structural properties.

TPSR experiments under non-catalyzed conditions have shown that gas-phase reactions between NO_2 and ethanol increase the availability of acetaldehyde in the vicinity of the catalyst bed at SCR temperatures through the formation/decomposition of ethylnitrite, the latter reaction being also catalyzed by the acid sites of SCZ materials. As deduced from TPSR data, the sulfation treatment improved the SCR activity, namely through the promotion of alternative pathways for the formation of N_2 and the inhibition of combustion reactions at medium temperatures. NOx conversions measured under TPSR and steady-state conditions (1920 ppm NO + 3020 ppm C_2H_5OH + 5% O_2) were shown to be superior to 30% on most of the SCZ catalysts between 250 and 400 °C. Above 350–400 °C, the selectivity was close to 100% for N_2 (HCN and N_2O were also formed at lower temperatures) and a maximal DeNOx yield of 48% was obtained for a sulfated catalyst with a Ce molar fraction of 0.5. The SCR-active sites on SCZ materials could possibly consist of $[Ce(O,Zr)_n\cdots H]^{x+}$ adducts in the vicinity of a sulfate or bisulfate species. The intrinsic activity of Ce sites was found to be slightly higher when associated with tetragonal structures (or intermediate compositions) than with cubic ones (Ce-rich compositions). By contrast, the sulfated zirconia catalyst with a monoclinic structure was found to be almost completely inactive under the same conditions.

Acknowledgements

This work has been done within the frame of the international research group (GDRI) on Environmental Catalysis and Sustainable Development (2006–2010, CNRS-PAN). We also greatly thank Rhodia-France for supplying the parent ceria–zirconia samples.

References

[1] P. Forzatti, L. Lietti, E. Tronconi, Nitrogen oxides removal, in: I.T. Horvath (Ed.), Industrial Encyclopedia of Catalysis, Wiley, New York, 2002.
[2] R.H. Heck, R.J. Farrauto, S.T. Gulati, Catalytic Air Pollution Control, 2nd edition, John Wiley & Sons, New York, 2002.
[3] C. Enderle, G. Vent, M. Paule, F. Duvinage, SAE Tech. Paper 2008-01-1182 (2008).
[4] Dieselnet, http://www.dieselnet.com (2009).
[5] R. Burch, J.P. Breen, F.C. Meunier, Appl. Catal. B 39 (2002) 283.
[6] R. Mital, S.C. Huang, B.J. Stroia, R.C. Yu, SAE Tech. Paper No. 2002-01-0956 (2002).
[7] N.W. Cant, I.O.Y. Liu, Catal. Today 63 (2000) 133.
[8] H. Akama, K. Matsushita, Catal. Surv. Jpn. 3 (1999) 139.
[9] V.I. Parvulescu, P. Grange, B. Delmon, Catal. Today 46 (1998) 233.
[10] G. Djéga-Mariadassou, Catal. Today 90 (2004) 27.
[11] Y.H. Yeom, M. Li, W.M.H. Sachtler, E. Weitz, J. Catal. 246 (2007) 413.
[12] Y.H. Yeom, M. Li, W.M.H. Sachtler, E. Weitz, J. Catal. 238 (2006) 100.
[13] Y.H. Yeom, M. Li, A. Savara, W.M.H. Sachtler, E. Weitz, Catal. Today 136 (2008) 55.
[14] M. Adamowska, S. Muller, P. Da Costa, A. Krzton, P. Burg, Appl. Catal. B: Environ. 74 (2007) 278.
[15] L. Zenboury, B. Azambre, J.V. Weber, Catal. Today 137 (2008) 167.
[16] A. Trovarelli, Catalysis by ceria and related materials, Catal. Sci. Ser., vol. 2, Imperial College Press, London, 2002.
[17] M. Waqif, P. Bazin, O. Saur, J.C. Lavalley, G. Blanchard, O. Touret, Appl. Catal. B: Environ. 11 (1997) 195.
[18] B. Azambre, L. Zenboury, J.V. Weber, P. Burg, Appl. Surf. Sci. 256 (2010) 4570.
[19] B. Azambre, L. Zenboury, P. Da Costa, F. Delacroix, S. Carpentier, A. Westermann, Catal. Today, submitted for publication.
[20] B. Azambre, L. Zenboury, A. Koch, J.V. Weber, J. Phys. Chem. C 113 (2009) 13287.
[21] B.M. Reddy, P.M. Sreekanth, P. Lakshmanan, A. Khan, J. Mol. Catal. A: Chem. 244 (2006) 1.
[22] C. Morterra, G. Cerrato, F. Pinna, M. Signoretto, J. Catal. 157 (2009) 109.
[23] I. Atribak, B. Azambre, A. Bueno López, A. García-García, Appl. Catal. B: Environ. 92 (2009) 126.
[24] G.D. Yadav, J.J. Neir, Micropor. Mesopor. Mater. 33 (1999) 1.
[25] M. Abián, S.L. Silva, A. Millera, R. Bilbao, M.U. Alzueta, Fuel Process Technol. 91 (2010) 1204.
[26] C. Binet, M. Daturi, J.C. Lavalley, Catal. Today 50 (1999) 207.
[27] R.L. Martins, L. Schmal, Appl. Catal. A: Gen. 308 (2006) 143.
[28] O. Kröcher, M. Elsener, Appl. Catal. B: Environ. 92 (2009) 75.
[29] E. Mamontov, R. Brezny, M. Koranne, T. Egami, J. Phys. Chem. B 107 (2003) 13007.